ChemComm

Accepted Manuscript

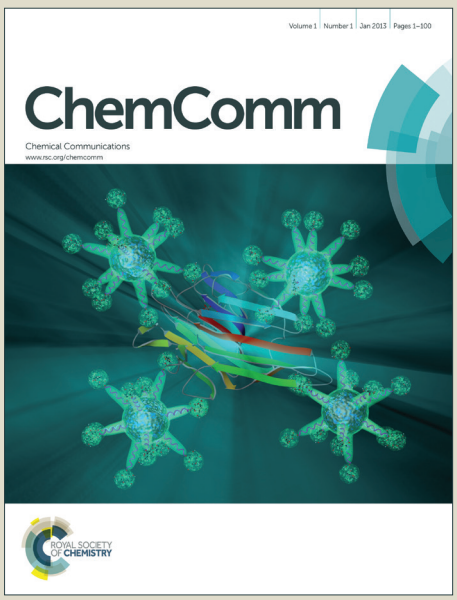

ROYAL SOCIETY OF CHEMISTRY

www.rsc.org/chemcomm

Cite this: DOI: 10.1039/c0xx00000x

www.rsc.org/xxxxxx

ARTICLE TYPE

$NaYF_4$:Yb,Er/MoS_2: from synthesis, surface ligands-stripping, to negative infrared photoresponse

Wenbin Niu,[a,b‡] Hu Chen,[b‡] Rui Chen,[c] Jingfeng Huang,[b] Handong Sun[c] and Alfred Iing Yoong Tok*[b]

Received (in XXX, XXX) Xth XXXXXXXXX 20XX, Accepted Xth XXXXXXXXX 20XX

DOI: 10.1039/b000000x

The synthesis, surface ligands-stripping, and infrared optoelectronic device application of $NaYF_4$:Yb,Er-MoS_2 nanocomposites are reported. $NaYF_4$:Yb,Er-MoS_2 film shows unusual negative infrared photoresponse after $SOCl_2$/DMF treatment, which demonstrates more than 2 times photoresponsivity than pure $NaYF_4$:Yb,Er, showing great potential for the development of novel infrared optoelectronic devices.

Nanocomposites have attracted great attention in recent years because of their composition-dependent properties.[1] Multicomponent nanomaterials containing two or more nanoscale components often exhibit multiple functionalities, and the interaction between the components in such system may provide the functionality that extend beyond those of isolated materials and even exhibit novel properties, thus achieving potential applications in catalysis, optoelectronic and photovoltaic devices.[2] As a layered transition chalcogenide material, MoS_2 has shown great promise for the future electronic and catalytic applications in virtue of their unique structures, electrical and optical properties.[3] In particular, the direct bandgap of mono- or few-layer MoS_2 suggests that it could be a promising material for optoelectronic applications.[4] For example, MoS_2 nanosheet exhibits a high channel mobility (~200 $cm^2V^{-1}s^{-1}$), photoresponsivity (880 AW^{-1}) and current On/Off ratio (10^{-8}) in a phototransistor.[4b,4c] However, the current MoS_2 optoelectronic devices show low if not negligible photoresponsivity to the light with wavelength >680 nm due to the weak absorption and intrinsic bandgap of MoS_2 nanosheet.[4b-e] Therefore, it is essential to extend the device photoresponse to long wavelength region, to broaden its applicability.

On the other hand, upconversion nanoparticles, particularly lanthanide-doped rare-earth nanocrystals, are capable of absorbing infrared irradiation and emit high-energy photons due to the special configuration of 4f electrons in rare-earth elements.[5] Among various upconversion materials, hexagonal $NaYF_4$:Yb,Er has been recognized as one of the most efficient UCNPs, showing potential applications in electronic devices, remote control devices and bioimaging.[2,6] However, studies on the nanocomposite of $NaYF_4$:Yb,Er and MoS_2 nanosheet for optoelectronic device applications are still absent so far. In this paper, we present successful synthesis of $NaYF_4$:Yb,Er UCNPs-MoS_2 nanocomposites by a two-step thermolysis method in a mixture of oleic acid (OA) and oleylamine (OM) as described in experimental section. Then, a new method of $SOCl_2$/DMF treatment was introduced to remove surface ligands of as-prepared materials for optoelectronic device application (Scheme 1). Photoresponse measurements revealed that these devices exhibited unusual negative photoresponsivity to infrared light, and $NaYF_4$:Yb,Er UCNPs-MoS_2 demonstrated much larger negative photoresponsivity than pure UCNPs.

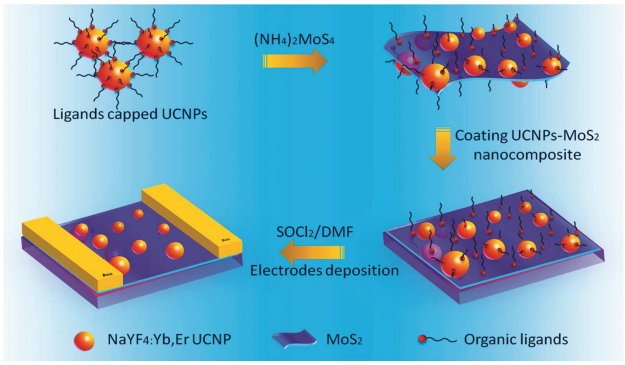

Scheme 1 Schematic illustration of the synthesis of $NaYF_4$:Yb,Er UNCPs -MoS_2 nanocomposites and the fabrication of photoresponse devices.

Fig. 1 shows transmission electron microscopy (TEM) images of $NaYF_4$:Yb,Er UCNPs, MoS_2, and UNCPs-MoS_2 nanocomposites with a molar ratio of 1/0.2 of UNCPs/MoS_2. $NaYF_4$:Yb,Er UCNPs used for the synthesis of nanocomposites were monodispersed in spherical shape with a size of around 16 nm as shown in Fig. 1a. The prepared pure MoS_2 was in sheet nanostructure with few layers (Fig. 1b and S1†). Fig. 1c-e show typical TEM images of the obtained UCNPs-MoS_2 nanocomposites. It can be observed that UCNPs were anchored on MoS_2 nanosheets, and most of them were wrapped by loosely few layered MoS_2 as indicated by arrows in Fig. 1c-1d and S2 (ESI†). The average size of $NaYF_4$:Yb,Er particles were slightly increased to ~18 nm and some of them were in rod and irregular shape with multi-crystallite . This variation mainly resulted from Oswald ripening and coalescence growth at high temperature during the synthesis of composites.[7] High resolution TEM (HRTEM) images (Fig. 1d and 1e) reveal lattice spacings of 0.3 and 0.65 nm, corresponding to the (110) facet of $NaYF_4$:Yb,Er and the (002) facet of MoS_2 sheet, respectively, indicating the anchor of UCNPs on MoS_2 nanosheets. As-prepared $NaYF_4$:Yb,Er-MoS_2 nanocomposites were also characterized by powder X-ray diffraction (XRD). The diffraction peaks and

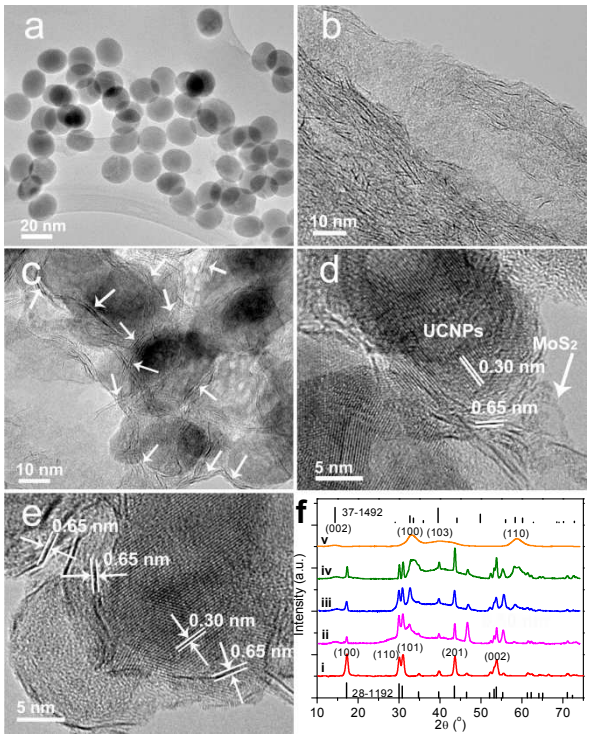

Fig. 1 TEM images of (a) $NaYF_4$:Yb,Er, (b) MoS_2, (c) $NaYF_4$:Yb,Er-MoS_2 (1/0.2), and (d, e) HRTEM images of nanocomposites. (f) XRD patterns of (f-i) $NaYF_4$:Yb,Er, (f-v) MoS_2, and $NaYF_4$:Yb,Er-MoS_2 nanocomposites prepared with different molar ratios of UNCPs/MoS_2: (f-ii) 1/0.1, (f-iii) 1/0.2, (f-iv) 1/0.4.

intensities of pure $NaYF_4$:Yb,Er (Fig. 1f-i) match well with the standard pattern of hexagonal phase (JCPDS: 28-1192).[5,6] For pure MoS_2, there are the broaden peaks of (101), (103), (110) lattice planes (JCPDS: 37-1492),[8] while the peak of (002) plane is weak, suggesting the predominated formation of few-layer MoS_2,[8] which agrees well with TEM result. As for UNCPs-MoS_2 composites, all samples showed the characteristic peaks of both $NaYF_4$:Yb,Er and MoS_2, and the peaks intensities of MoS_2 [e.g. (100), and (110)] gradually increased with increasing MoS_2 ratio (Fig. 1f-i-iv). In addition, the relatively higher emission of a physical mixture of UCNPs and MoS_2 than their nanocomposite (Fig. S4†) further imply the close contact between $NaYF_4$:Yb,Er and MoS_2. Otherwise, UCNPs-MoS_2 nanocomposites would give the same spectrum as that of their mixture (Fig. S4†). Furthermore, the excellent stability of the nanocomposites after surface ligands-removal (discussed below) further implies the strong interaction between UCNPs and MoS_2 nanosheets. Therefore, in combination with HRTEM images, XRD and upconversion spectra, these results indicate the formation of $NaYF_4$:Yb,Er-MoS_2 nanocomposites.

Fig. 2a exhibits the upconversion emission spectra of the corresponding samples. It can be clearly observed that the characteristic emission bands of Er^{3+} ion were centred at 410, 520, 540 and 660 nm resulting from $^4H_{9/2}\rightarrow{}^4I_{15/2}$, $^2H_{11/2}\rightarrow{}^4I_{15/2}$, $^4S_{3/2}\rightarrow{}^4I_{15/2}$ and $^4F_{9/2}\rightarrow{}^4I_{15/2}$ transitions, respectively. The composite samples show a reduction in emission intensity in comparison with pure $NaYF_4$:Yb,Er, and the intensity of emission peaks decreased further with increasing the amount of MoS_2 in the samples. This is because the strong absorption of MoS_2 at a

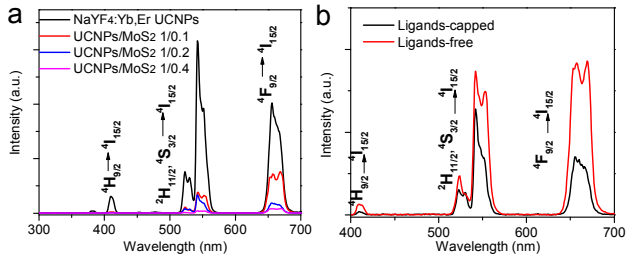

Fig. 2 Upconversion luminescence spectra of (a) $NaYF_4$:Yb,Er-MoS_2 composites with various molar ratios, and (b) $NaYF_4$:Yb,Er-MoS_2 (1/0.2) before and after ligands removal.

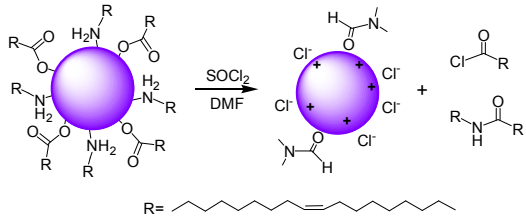

Scheme 2. Reactive ligands stripping of carboxylate- and amine-passivated nanomaterials with $SOCl_2$/DMF.

broad wavelength range from 300 to 700 nm covers emissions of $NaYF_4$:Yb,Er UCNPs (Fig. S5†). The reduced lifetime indicates the existence of fluorescence resonance energy transfer and/or charge transfer procedure in nanocomposites (Fig. S6†). According to the data extracted, the energy-transfer efficiency of the composite is determined to be round 0.16, indicating radiative energy transfer due to photon re-absorption also take places.

In most cases, long hydrocarbon molecules containing a coordinating headgroup such as OA and OM were employed as surfactant ligands for controlled synthesis and stabilization of high-quality nanomaterials. The presence of these large organic molecules, however, creates an insulating shell around the surface, thus blocking charge transport and limiting their applications in electronic and optoelectronic devices.[9] It is therefore necessary to remove these long-chain insulating ligands for practical device applications. In this work, a new approach for the removal of surface native ligands of as-prepared nanomaterials by using $SOCl_2$/DMF (namely Vilsmeier Reagent) is also presented, which can be completed in 2 min. $SOCl_2$ is a well-known chloridization agent, and can readily react with carboxylic acid, amine, alcohol *etc*. DMF is used as a catalyst to activate $SOCl_2$ and accelerate the reaction with surface ligands,[10] thus achieving rapid removal of native ligands (Scheme 2). In the case that only $SOCl_2$ was added to the hexane dispersion of nanoparticles, no apparent precipitation was found even after ultrasonication for several minutes. On the contrary, rapid precipitation of nanoparticles were observed after addition of two drops of DMF with gentle shaking, indicating a dramatic change in material solubility as a result of induced surface modification.

Fourier transform infrared (FT-IR) spectra of the samples (Fig. 3) confirmed the removal of surface ligands. As expected, all samples before $SOCl_2$/DMF treatment exhibited strong characteristic absorption bands of alkyl chains of OA and OM (Fig. 3a-c): the asymmetric and symmetric stretching vibrations of methylene (CH_2 at 2924 and 2853 cm^{-1}, respectively) and carboxyl groups (COO-) at around 1564 cm^{-1}.[11] After treatment with $SOCl_2$/DMF, these signals were absent, confirming

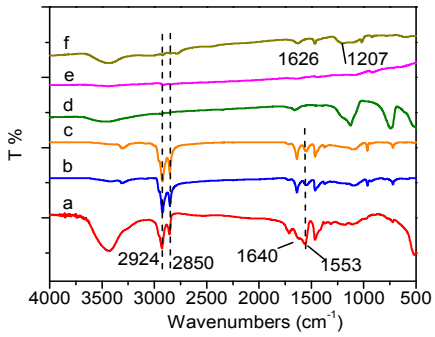

Fig. 3 FT-IR spectra of ligands-capped $NaYF_4$:Yb,Er, MoS_2, and $NaYF_4$:Yb,Er-MoS_2 composites before (a, b and c) and after (d, e and f) $SOCl_2$/DMF treatment, respectively.

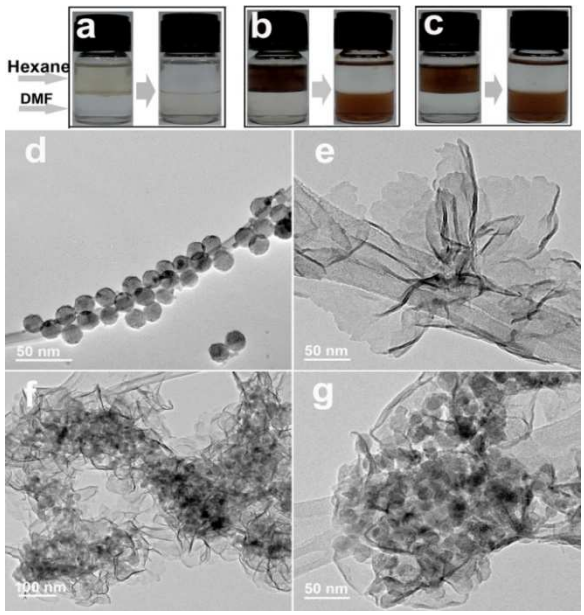

Fig. 4 Illustration of the phase-transfer of (a) $NaYF_4$:Yb,Er, (b) MoS_2, and (c) $NaYF_4$: Yb,Er-MoS_2 composites (1/0.2) from nonpolar solvent (hexane) to polar solvent (DMF) before and after $SOCl_2$/DMF treatment, and the corresponding TEM images of (d) $NaYF_4$:Yb,Er, (e) MoS_2 and (f, g) $NaYF_4$:Yb,Er-MoS_2 composites (1/0.2) dispersed in DMF after surface ligands removal.

complete removal of organic surfactants from nanomaterial surface. The resulting precipitate can be well redispersed in polar solvent such as DMF and DMSO (Fig. 4a-4c). Fig. 4d-4f exhibits the corresponding TEM images. For UCNPs, the size and shape were preserved after treatment, and no obvious aggregation was observed upon surface modification (Fig.S7†). The shape of MoS_2 was slightly changed after treatment, and no initially loose layers were shown (Fig. 4e and S8†). Notably, the removal of organic ligands led to the variation of upconversion emission. For example, as compared to the untreated $NaYF_4$:Yb,Er-MoS_2 composite (1/0.2), all emission intensities of $^4H_{9/2}\rightarrow{}^4I_{15/2}$, $^2H_{11/2}$, $^4S_{3/2}\rightarrow{}^4I_{15/2}$ and $^4F_{9/2}\rightarrow{}^4I_{15/2}$ transitions in modified composites were much higher (Fig. 2b). This is because the removal of organic ligands with long-alkyl chain reduces the nonradiative relaxation of excited Er^{3+} ion from $^2H_{11/2}/^4S_{3/2}$ to $^4F_{9/2}$ and $^4I_{11/2}$ to $^4I_{13/2}$ levels (Fig. S9),[11] thus enhancing emission intensities. The successful stripping and redispersion of UCNPs, MoS_2 nanosheet and their composites passivated by either oleate or amine ligands imply the potential applications of this method for a variety of

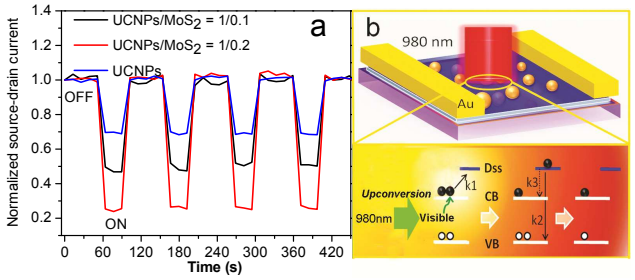

Fig. 5 (a) Real-time measurements of the normalized drain current of infrared photoresponse devices while the 980 nm infrared light is switched on and off with V_{DS} 10 mV at zero gate bias. UCNPs and UCNPs/MoS_2 (1/0.1, 1/0.2) represent the devices prepared with $NaYF_4$:Yb,Er UCNPs and $NaYF_4$:Yb,Er-MoS_2 composite (1/0.1, 1/0.2) films treated with hexane solution of $SOCl_2$/DMF. (b) Schematic illustration of the device and the proposed mechanism of negative infrared photoresponse.

nanocrystals with different sizes, shapes, and surface ligands. Instead of tetrafluoroborates and metal chalcogenide complexes reported before,[9,12] readily available $SOCl_2$/DMF is employed in this work, which was demonstrated to be a facile, rapid and efficient approach for the removal of native ligands while leaving the surface of nanomaterial bare and hydrophilic.

To demonstrate infrared photodetector application, photoresponse devices with the corresponding materials were fabricated. The photoresponses of these devices upon 980 nm infrared light irradiation were investigated. For the device fabrication, the films of surfactant ligands-capped nanomaterials were deposited on substrate, followed by immersion in a dilute solution of $SOCl_2$/DMF in hexane to remove the insulating organic ligands. Lastly, gold electrodes were deposited on top. Due to efficient removal of insulating ligands, favorable effect on the optoelectronic properties of the treated films is anticipated. Fig. 5a shows the time-dependent normalized drain current of the devices with a source-drain voltage (V_{DS}) of 10 mV at zero gate bias. Importantly, different from usually observed positive photocurrent response in semiconductor nanomaterials, unexpected *negative* photoresponse were exhibited in their films upon 980 nm infrared light irradiation (Fig. 5a, S10 and S11, ESI†). Once the incident light was removed, the current jumped back to the baseline level. Specifically, the photoresponse device with pure UCNPs exhibited 30% decrease in I_d. For UCNP-MoS_2 nanocomposites, the device with a ratio of 1/0.1 of UCNP/MoS_2 exhibited a 50% decrease in source-drain current, and the one with a molar ratio of 1/0.2 showed up to 75% decrease (Fig. 5a), while no source-drain current was measured for 1/0.4 nanocomposite and pure MoS_2, due to the large cracks induced by the reduction of inter-nanosheet spacing after $SOCl_2$/DMF treatment (Fig. S12†).[12a] It was indicated that the presence of MoS_2 in nanocomposites led to a stronger negative photoresponse, however, an excess amount of MoS_2 resulted in the formation of large cracks in the films after $SOCl_2$/DMF treatment, as a result, no source-drain current was measured.

Recently, Talapin *et al.* proposed a model to explain the negative photoconductivity in InAs nanocrystal film,[9c] in which donorlike state form a localized level (D_{ss}) presumably located above the mobility edge. Photo-induced trapping of mobile electrons on this localized level (D_{ss}) resulted in negative photoconductivity. Such donorlike surface state has been

observed in semiconductor nanocrystals.[13] This model is also a reasonable explanation for the experimentally observed negative photoresponses in this work (See ESI† for more details). We presume that the donorlike surface state is also formed in UCNPs and MoS_2 after surface treatment and locate above the mobility edge (Figure 5b). Upon 980 nm irradiation, a mobile electron is excited and gets trapped at D_{ss} level (k1), resulting in decreased conductivity. The electron trapped in D_{ss} state can either nonradiatively recombine with a hole in valence band (k2, VB) or relax into the conduction band (k3, CB). When infrared light is off, electrons are no longer trapped and the conductivity is restored. Increasing the ratio of MoS_2 in hybrid composites may increase D_{ss} surface state due to the large specific area of nanosheet structure, thus causing stronger negative photoresponse. The detailed mechanism is still under investigation.

In summary, the synthesis, surface ligands-stripping, and negative infrared photoresponse of new $NaYF_4$:Yb,Er UCNPs-MoS_2 nanocomposites were demonstrated. The synthesis of composites was achieved by thermolysis method in organic surfactant ligands. Then, we presented a new method using $SOCl_2$/DMF treatment to remove surface ligands of these nanomaterials for device applications, which was demonstrated to be a facile, rapid yet efficient approach for complete removal of native ligands, showing potential applications for a variety of nanocrystals. Most importantly, after $SOCl_2$/DMF treatment, UCNPs-MoS_2 nanocomposites films exhibited unexpected negative photoresponses to 980 nm illumination, and the photoresponsivity of UCNPs-MoS_2 (1/0.2) was more than two times of that of pure UCNPs, indicating the potential application of these materials in infrared photoresonse devices. Also, this negative photoresponse phenomenon provides the opportunity for the development of novel optoelectronic devices.

Notes and references

[a] *State Key Laboratory of Fine Chemicals, Dalian University of Technology, West Campus, 2 Linggong Rd., Dalian 116024, China*
[b] *School of Materials Science and Engineering, Nanyang Technological University, 50 Nanyang Avenue, 639798, Singapore. E-mail: MIYTok@ntu.edu.sg*
[c] *Division of Physics and Applied Physics, School of Physical and Mathematical Sciences, Nanyang Technological University, 21 Nanyang Link, 637371 Singapore.*

† Electronic Supplementary Information (ESI) available: Experimental section, HRTEM of MoS_2, TEM, SEM and absorbance spectra of ligands-capped UCNPs-MoS_2 nanocomposites, upconversion spectra and TEM images of ligands-free UCNPs-MoS_2, upconversion mechanism and infrared photoresponse measurements of nanocomposites. See DOI: 10.1039/b000000x/

‡ These authors contributed equally to this work.

1 a) A. G. Dong, J. Chen, P. M. Vora, J. M. Kikkawa and C. B. Murray *Nature* 2010, **466**, 474; b) P. Li, Z. Wei, T. Wu, Q. Peng and Y. D. Li, *J. Am. Chem. Soc.* 2011, **133**, 5660.
2 L. Cheng, K. Yang, Y. G. Li, J. H. Chen, C. Wang, M. W. Shao, S. T. Lee and Z. Liu *Angew. Chem. Int. Edit.* 2011, **50**, 7385.
3 a) F. K. Meng, J. T. Li, S. K. Cushing, M. J. Zhi and N. Q. Wu, *J. Am. Chem. Soc.* 2013, **135**, 10286; b) Q. J. Xiang, J. G. Yu and M. Jaroniec *J. Am. Chem. Soc.* 2012, **134**, 6575; c) J. Yang, D. Voiry, S. J. Ahn, D. Kang, A. Y. Kim, M. Chhowalla and H. S. Shin, *Angew. Chem. Int. Edit.* 2013, **52**, 13751.
4 a) M. Chhowalla, H. S. Shin, G. Eda, L. J. Li, K. P. Loh and H. Zhang *Nat. Chem.* 2013, **5**, 263; b) O. Lopez-Sanchez, D. Lembke, M. Kayci, A. Radenovic and A. Kis *Nat. Nanotechnol.* 2013, **8**, 497; c) Z. Y. Yin, H. Li, H. Li, L. Jiang, Y. M. Shi, Y. H. Sun, G. Lu, Q. Zhang, X. D. Chen and H. Zhang *Acs Nano* 2012, **6**, 74; d) S.H. Su, Y. T. Hsu, Y. H. Chang, M. H. Chiu; C. L. Hsu, W. H. Chang, J. H. He and L. J. Li *Small* 2014, **10**, 2589.
5 a) L. Cheng, C. Wang, X. X. Ma, Q. L. Wang, Y. Cheng, H. Wang, Y. G. Li and Z. Liu *Adv. Funct. Mater*. 2013, **23**, 272; b) D. Chen, Y. Yu, F. Huang, A. Yang and Y.S. Wang *J. Mater. Chem.* 2011, **21**, 6186; c) F. Wang and X. G. Liu *J. Am. Chem. Soc.* 2008, **130,** 5642; d) X. J. Xie, N. Y. Gao, R. R. Deng, Q. Sun, Q. H. Xu and X. G. Liu *J. Am. Chem. Soc*. 2013, **135**, 12608; e) D. Li, Q. Shao, Y. Dong and J. Jiang *Chem. Commun*., 2014, **50**, 15316; f) Z. Yin, Y. Zhu, W. Xu, J. Wang, S. Xu, B. Dong, L. Xu, S. Zhang and H. Song *Chem. Commun.*, 2013, **49**, 3781; g) Y. S. Liu, D. T. Tu, H. M. Zhu, R. F. Li, W. Q. Luo and X. Y. Chen, *Adv. Mater.* 2010, **22**, 3266; h) N. Bogdan, F. Vetrone, G. A. Ozin and J. A. Capobianco *Nano. Lett*. 2011, **11**, 835; i) F. Wang, L. D. Sun, J. Gu, Y. F. Wang, W. Feng, Y. Yang, J. F. Wang and C. H. Yan *Angew. Chem. Int. Edit.* 2012, **51**, 8796; j) W. B. Niu, L. T. Su, R. Chen, H. Chen, Y. Wang, A. Palaniappan, H. D. Sun and A. L. Y. Tok *Nanoscale* 2014, **6**, 817.
6 a) B. Dong, S. Xu, J. Sun, S. Bi, D. Li, X. Bai, Y. Wang, L. Wang and H. Song *J. Mater. Chem*., 2011, **21**, 6193; b) Y. Liu, M. Chen, T. Y. Cao, Y. Sun, C. Y. Li, Q. Liu, T. S. Yang, L. M. Yao, W. Feng and F. Y. Li *J. Am. Chem. Soc.* 2013, **135,** 9869; c) C. L. Zhang, Y. X. Yuan, S. M. Zhang, Y. H. Wang and Z. H. Liu *Angew. Chem. Int. Edit.* 2011, **50**, 6851; d) Z. Y. Hou, C. X. Li, P. A. Ma, G. G. Li, Z. Y. Cheng, C. Peng, D. M. Yang, P. P. Yang and J. Lin *Adv. Funct. Mater*. 2011, **21,** 2356; e) W. Li, J. S. Wang, J. S. Ren and X. G. Qu *J. Am. Chem. Soc*. 2014, **136**, 2248; f) Y. L. Dai, H. H. Xiao, J. H. Liu, Q. H. Yuan, P. A. Ma, D. M. Yang, C. X. Li, Z. Y. Cheng, Z. Y. Hou, P. P. Yang and J. Lin *J. Am. Chem. Soc*. 2013, **135**, 18920; g) S. Wang, L. Zhang, C. Dong, L. Su, H. Wang and J. Chang *Chem. Commun*., 2015, **51**, 406. h) Q. Kong, L. Zhang, J. Liu, M. Wu, Y. Chen, J. Feng and J. Shi *Chem. Commun*., 2014, **50**, 15772; i) Y. Wu, Y. Cen, L. Huang, R. Yu and X. Chu *Chem. Commun*., 2014, **50**, 4759; j) J. Chang, Y. Ning, S. Wu, W. Niu and S. Zhang *Adv. Funct. Mater*. 2013, **23**, 5910.
7 a) N. J. J. Johnson, A. Korinek, C. H. Dong and F. C. J. M. van Veggel *J. Am. Chem. Soc*. 2012, **134**, 11068; b) X. C. Ye, J. E. Collins, Y. J. Kang, J. Chen, D. T. N. Chen, A. G. Yodh and C. B. Murray *P Natl. Acad. Sci. USA* 2010, **107**, 22430; c) H. Zheng, R. K. Smith, Y. Jun, C. Kisielowski, U. Dahmen and A. P. Alivisatos, *Science*, 2009, **324**, 1309.
8 C. Altavilla, M. Sarno and P. Ciambelli *Chem. Mater*. 2011, **23**, 3879.
9 a) M. V. Kovalenko, M. Scheele and D. V. Talapin *Science* 2009, **324**, 1417; b) D. S. Chung, J. S. Lee, J. Huang, A. Nag, S. Ithurria and D. V. Talapin *Nano. Lett*. 2012, **12**, 1813; c) W. Y. Liu, J. S. Lee and D. V. Talapin *J. Am. Chem. Soc*. 2013, **135**, 1349.
10 a) A. Arrieta, J. M. Aizpurua and C. Palomo *Tetrahedron Lett.* 1984, **25**, 3365; b) F. Xu, B. Simmons, R. A. Reamer, E. Corley, J. Murry and D. Tschaen *J. Org. Chem*. 2008, **73**, 312.
11 a) W. B. Niu, S. L. Wu and S. F. Zhang *J. Mater. Chem*. 2011, **21**, 10894; b) W. B. Niu, S. L. Wu, S. F. Zhang, J. Li and L. Li *Dalton T.* 2011, **40**, 3305.
12 a) E. L. Rosen, R. Buonsanti, A. Llordes, A. M. Sawvel, D. J. Milliron and B. A. Helms *Angew. Chem. Int. Edit*. 2012, **51**, 684; b) A. G. Dong, X. C. Ye, J. Chen, Y. J. Kang, T. Gordon, J. M. Kikkawa and C. B. Murray *J. Am. Chem. Soc*. 2011, **133**, 998; c) S. D. Dmitry, N. Dirin, M. I. Bodnarchuk, G. Nedelcu, P. Papagiorgis, G. Itskos and M. V. Kovalenko *J. Am. Chem. Soc*. 2014, **136**, 6550.
13 a) M. Shim and P. Guyot-Sionnest, *Nature* 2000, **407**, 981; b) D. Y. Petrovykh, M. J. Yang and L. Whitman, *J. Surf. Sci.* 2003, **523**, 231.